ChemComm

COMMUNICATION

View Article Online
View Journal

Cite this: DOI: 10.1039/c5cc02732b

Received 1st April 2015,
Accepted 11th June 2015

DOI: 10.1039/c5cc02732b

www.rsc.org/chemcomm

Paramagnetic relaxation based biosensor for selective dopamine detection†

Tevhide Ozkaya Ahmadov, Padmanabh Joshi, Jinnan Zhang, Keaton Nahan, Joseph A. Caruso and Peng Zhang*

We report a new NMR relaxation time-based method for sensitive and selective dopamine detection using paramagnetic nanoparticles. The Fe^{3+} species in the nanoparticles serves as both the contrast agent and the target recognition element. The results demonstrate that paramagnetic nanoparticles, similar to the more widely used superparamagnetic nanoparticles, can be integrated into relaxation based detection schemes while avoiding the aggregation problem commonly associated with superparamagnetic nanoparticles.

One of the major challenges in biosensing is the accurate, selective and rapid detection of important targets, such as disease biomarkers, pathogens and cancer cells in biological samples, preferably with little or no pretreatment. Over the years different biosensing systems have been developed to detect such targets with good selectivity and sensitivity, enabling early disease diagnosis.[1–3] Among them, magnetic nanoparticles (MNPs) based biosensing has received considerable attention recently.[4–6] Magnetic relaxation switch (MRS) based sensing methods have shown good promise to provide fast and reliable results using benchtop nuclear magnetic resonance (NMR) relaxometer.[7–11] These methods are based on the use of surface-functionalized MNPs to recognize specific targets. The switch between a dispersed and clustered state of the MNPs upon interaction with the target lead to a change in the transverse relaxation time (T_2) of the water protons in the solution.[12,13]

Superparamagnetic iron oxide nanoparticles (SPION) are commonly used in MRS based sensing. Nevertheless, there are challenges associated with the target-induced clustering detection schemes, *e.g.*, over-clustering of nanoparticles will lead to their precipitation, undermining the reliability of T_2 measurement results. Thus, improvement in the stability of MNPs prior to and after target addition is crucial to the relaxation-based detection.

Paramagnetic metal ions, such as Gd^{3+}, Fe^{3+}, Mn^{2+}, Mn^{3+} and Cu^{2+}, can also affect the transverse (T_2) and longitudinal (T_1) relaxation times of the surrounding water protons, and serve as contrast agents in magnetic resonance imaging (MRI).[1,14–17] Due to the toxicological concerns on the free metal aqua ions, chelating ligands are commonly used to reduce the toxicity of the metal ions.[18–21] However, complete coordination of metal ions decreases the access of water protons to the metal ions, and the overall effectiveness of the metal ions as contrast agents decreases.[22,23] Therefore it is important to develop metal chelates with both strong magnetic relaxivity to act as good contrast agents and good stability to ensure low toxicity.[24,25] Gd^{3+} chelates have been the most frequently used contrast agents commercially because of their strong paramagnetic properties. Other more biocompatible paramagnetic metal chelates have also been investigated of viability as contrast agents.[26,27] Fe^{3+} ion has five unpaired electrons with high magnetic moment, thus is a good candidate for acting as contrast agent.[28] However, Fe^{3+} ions tend to form insoluble oxides at pH > 4. On the other hand, complete coordination of Fe^{3+} ions by ligands would greatly interfere with the interaction between Fe^{3+} ions and water protons, which largely reduces the efficiency of Fe^{3+}-based contrast agents.[28] Hence, one of the major challenges in developing Fe^{3+}-based contrast agents is to improve the stability and dispersibility of Fe^{3+} complexes in the aqueous media while maintaining the accessibility of the Fe^{3+} ions by water protons.[20,29]

Herein, we report the development of a T_2-based detection method for dopamine, an important neurotransmitter associated with various brain functions including learning and memory. Currently, there have been a number of methods reported on the detection of dopamine, such as, surface-enhanced Raman spectroscopy (SERS),[30–32] electrochemistry,[33] UV-vis spectroscopy[34] and fluorescent spectroscopy.[35] While these methods have shown varying degrees of success in detecting dopamine, there is ongoing need to develop alternative methods that are less labor-intensive, less time-consuming or expensive, and with little sample pretreatment. The detection described here can be carried out on a benchtop NMR relaxometer within minutes, and does not require sample pretreatment.

The principle of the sensing scheme is shown in Fig. 1. Ethyldiaminetriacetic acid groups (EDTA) are first grafted onto

Department of Chemistry, University of Cincinnati, Cincinnati, OH 45221, USA. E-mail: peng.zhang@uc.edu; Tel: +1 513-556-9222

† Electronic supplementary information (ESI) available: Experimental details. See DOI: 10.1039/c5cc02732b

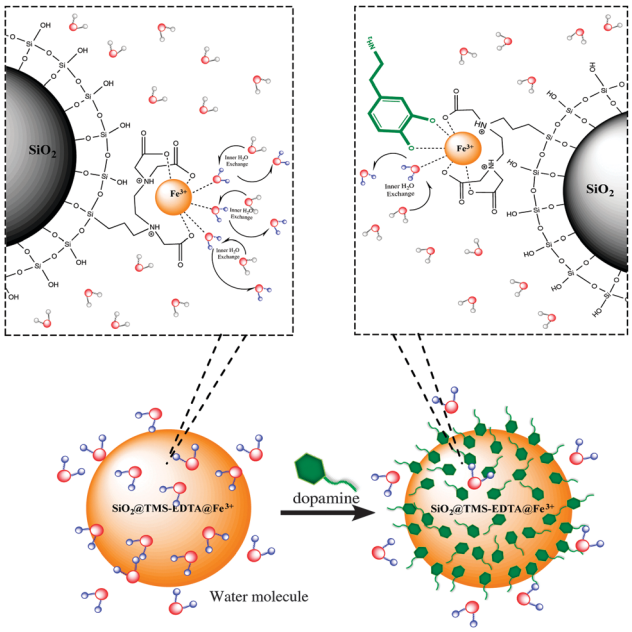

Fig. 1 Illustration of the detection scheme of the designed biosensor. Upon the addition of dopamine, SiO_2@TMS-EDTA@Fe^{3+} nanoparticles bind to dopamine, leading to increased T_2 relaxation time of the surrounding water protons.

the surface of silica nanoparticles (SiO_2 NPs) through the use of EDTA-functionalized silane. As strong chelating agents for many metal ions, the EDTA groups on the nanoparticle surface can readily capture and stabilize Fe^{3+} ions in aqueous solution, which would reduce the relaxation rate of water protons. Meanwhile, dopamine would bind to Fe^{3+} ions selectively due to the high affinity of its catechol groups to Fe^{3+},[32,36] and interfere with the interaction between the Fe^{3+} ions and water protons, subsequently affecting the relaxation rate of water protons in the solution.[19,37] Experimentally, by monitoring the T_2 of water protons, which is directly associated with the relaxation rate of water protons, we can detect the presence of dopamine.

SiO_2@TMS-EDTA nanoparticles were synthesized following a modified version of the previously published protocol while introducing the EDTA-functionalized silane (TMS-EDTA) to the microemulsion system.[38] Fe^{3+} ions can bind to the SiO_2@TMS-EDTA nanoparticles at low pH, which greatly simplifies the preparation process and eliminates the insoluble oxides formed by Fe^{3+} ions. Detailed experimental processes are provided in the ESI.†

The synthesized SiO_2@TMS-EDTA@Fe^{3+} nanoparticles were characterized by a number of techniques. The diameters of the SiO_2@TMS-EDTA nanoparticles were confirmed by transmission electron microscopy (TEM), which show an average diameter of ~60 nm (Fig. 2a). Results of dynamic light scattering (DLS) measurement (Table 1) are consistent with that of TEM. Chelation of SiO_2@TMS-EDTA with Fe^{3+} ions results in the change of zeta potential of SiO_2@TMS-EDTA nanoparticles. Nevertheless, zeta potentials of both SiO_2@TMS-EDTA and SiO_2@TMS-EDTA@Fe^{3+} nanoparticles indicate fairly good stability of the nanoparticles at pH 4 (Table 1). The amount of Fe^{3+} species in

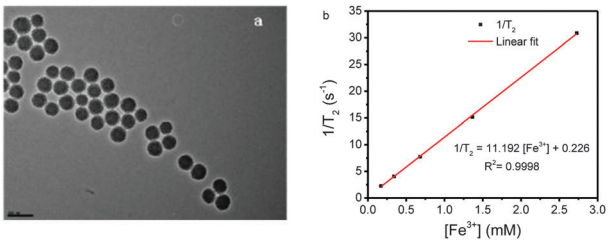

Fig. 2 (a) TEM image of the SiO_2@TMS-EDTA@Fe^{3+} nanoparticles. (b) R_2 relaxivity measurement of SiO_2@TMS-EDTA@Fe^{3+} nanoparticles in acetate buffer.

Table 1 Zeta potential and size of the nanoparticles measured by particle size analyzer

	Zeta potential (mV)	Size by DLS (nm)
SiO_2@TMS-EDTA	-53 ± 5	68.1 ± 0.7
SiO_2@TMS-EDTA@Fe^{3+}	-31 ± 3	65.5 ± 0.5

the SiO_2@TMS-EDTA@Fe^{3+} nanoparticle solution was quantified using ICP-MS and determined to be 0.228 μg mL^{-1}.

The binding of dopamine to the SiO_2@TMS-EDTA@Fe^{3+} nanoparticles is reflected by the change in the absorption spectrum. It has been reported that Fe^{3+}–dopamine complex in solution displays characteristic absorption peaks depending on the number and type of ligands. Additional chelation to Fe^{3+} ion by ligands results in peak shift in the absorption spectrum.[32] In this study, the SiO_2@TMS-EDTA@Fe^{3+}–dopamine complex has a dark green-blue color with a broad absorption band at ~650 nm. The color develops very quickly with high concentration of dopamine (Fig. S1, ESI†).

FTIR spectra of SiO_2@TMS-EDTA, and SiO_2@TMS-EDTA@Fe^{3+} nanoparticles were obtained to verify the surface functional groups by TMS-EDTA silane and the subsequent chelation with Fe^{3+}. As shown in Fig. 3b, a strong absorption band between 1000 and 1200 cm^{-1} indicate the presence of Si–O bands.[39] The absorption peaks at 1396 and 1633 cm^{-1} are attributed to the symmetric C–O stretching and the asymmetric C–O stretching vibrations after the TMS-EDTA treatment.[39] A weak asymmetric CH_2 stretching band can be observed at 2981 cm^{-1}. The broad band at 3100–3600 cm^{-1} comes from the O–H stretching vibrations.

Transverse relaxation times (T_2) of water protons were measured by a Bruker Minispec mq60 relaxometer operating at 1.41 Tesla and 40 °C without any washing step. The T_2 values

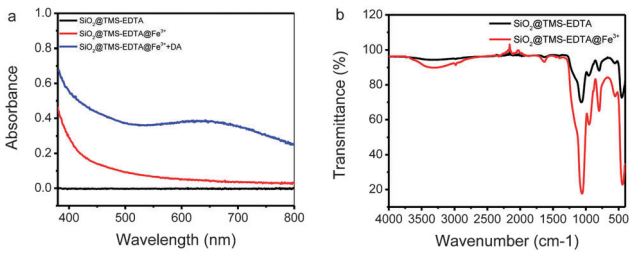

Fig. 3 (a) UV-vis and (b) FT-IR spectra of the SiO_2@TMS-EDTA and SiO_2@TMS-EDTA@Fe^{3+} nanoparticles with dopamine.

of the SiO_2@TMS-EDTA@Fe^{3+} nanoparticles in aqueous solution result in the transverse relaxivity of the nanoparticles, R_2 = 11.19 mM^{-1} s^{-1}, as plotted in Fig. 2b. This R_2 value is comparable to that of Fe^{3+} ions reported in the literature.[28]

The percentage change of T_2 relaxation time (ΔT_2%) upon the binding of dopamine to SiO_2@TMS-EDTA@Fe^{3+} nanoparticles is calculated according to the following equation:[40,41]

$$\Delta T_2\% = (T_{2\,\text{target}} - T_{2\,\text{blank}}) \times 100/T_{2\,\text{blank}}$$

where $T_{2\,\text{blank}}$ and $T_{2\,\text{target}}$ is the average T_2 relaxation time of three replicates of nanoparticle solution before and after dopamine addition, respectively.

We first tested the detection of dopamine in acetate buffer. As shown in Fig. 4a, a continuous increase in ΔT_2% is observed as the dopamine concentration rises up to 80 μM. A linear relationship between ΔT_2% and dopamine concentration exists in the range of 1–10 μM with a correlation coefficient (R^2) of 0.995 and a detection limit of 0.2 μM.

To assess the specificity of this detection scheme, comparison experiments using glucose and sucrose as potential dopamine competitors of comparable concentrations were carried out. Results shown in Fig. S2 of the ESI† demonstrate that these sugar molecules do not significantly affect the detection of dopamine. Furthermore, dopamine present in a complex matrix, an Artificial Cerebrospinal Fluid (aCSF), was used as the sample. The aCSF is a complex mixture simulating the easily accessible fluid in the ventricular system. It contains several salts and sugars: 124 mM NaCl, 2.5 mM KCl, 2.0 mM $MgSO_4$, 1.25 mM KH_2PO_4, 26 mM $NaHCO_3$, 10 mM glucose, 4 mM sucrose, and 2.5 mM $CaCl_2$.[30] Results shown in Fig. 4b demonstrate that, even at the relatively high concentrations of various salts and sugars, the SiO_2@TMS-EDTA@Fe^{3+} nanoparticles can still detect dopamine quantitatively. A linear relationship between dopamine concentration in aCSF and ΔT_2% is observed for the same dynamic range of 1–10 μM and a detection limit of 0.5 μM. Since the aCSF contains millimolar concentrations of sugars, it is expected that the slight increase in the uncertainty of ΔT_2% measurement by the presence of sugars in samples would be reduced with aCSF as the solvent matrix, as compared to the case of using acetate buffer as the solvent matrix (Fig. S2, ESI†). The results illustrate the capability of detecting dopamine in the complex matrix quantitatively, without the need of sample pretreatment.

It is worthwhile to point out a couple of important features in this nanoparticle-based design of sensing. The SiO_2 component of the SiO_2@TMS-EDTA@Fe^{3+} nanoparticles appears to be critical in creating a change of the T_2 value of water protons before and after the dopamine binding. It is well known that free Fe^{3+} ions can bind to dopamine in solution. Yet the T_2 value of water protons in solution containing only free Fe^{3+} ions is unstable, which cannot be used to signal the presence of dopamine. In contrast, the T_2 value of water protons in solution containing SiO_2@TMS-EDTA nanoparticles is very stable. The synthesized SiO_2@TMS-EDTA@Fe^{3+} nanoparticles have excellent water dispersibility and colloidal stability in the acidic buffer. The presence of carboxyl and hydroxyl groups on the surface of SiO_2@TMS-EDTA nanoparticles prevents their aggregation, which tends to be a common issue with superparamagnetic nanoparticles, and provides good stability over weeks without any precipitation. To the other end, in many Fe^{3+}-ligand complexes the Fe^{3+} ion usually has a coordination number of 6, which prevents either the binding of dopamine to the Fe^{3+}-center or the direct interaction between water protons and the Fe^{3+}-center.[42] Thus the T_2 value of water protons in solution containing only Fe^{3+}-ligand complexes, such as Fe-EDTA, barely changes upon the dopamine addition. TMS-EDTA is a pentadentate ligand,[43] and has less coordination sites for metal center at low pH, resulting in more available coordination sites on the Fe^{3+} ion to interact with dopamine and water protons.[44] The SiO_2 nanoparticle and TMS-EDTA combine to serve well as a platform for the paramagnetic relaxation based sensing.

The Fe^{3+} species of the SiO_2@TMS-EDTA@Fe^{3+} nanoparticles in this scheme has two functions: (1) it is the paramagnetic agent that directly causes change to the T_2 relaxation time of the surrounding water protons; (2) it is the target recognition element that selectively binds to dopamine. Moreover, by immobilizing other target recognition elements on the nanoparticle surface, the SiO_2@TMS-EDTA@Fe^{3+} nanoparticles can be adapted to detect other targets that do not directly bind to the Fe^{3+} species.

In summary, we have demonstrated a T_2-based detection method for dopamine using paramagnetic nanoparticles. Detection limits of sub-micromolar concentration are achieved for dopamine in both acetate buffer and aCSF matrix without sample pretreatment.

This work was partially supported by the National Science Foundation (CBET-1065633).

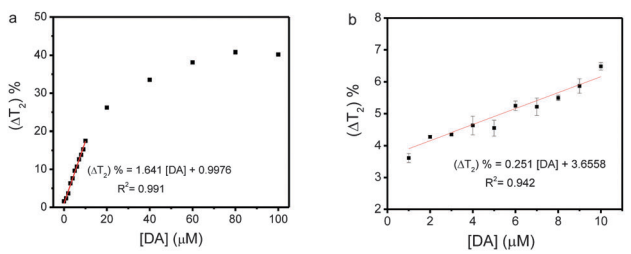

Fig. 4 ΔT_2% as a function of dopamine concentration with samples in (a) acetate buffer, and (b) aCSF.

Notes and references

1 J. B. Haun, T. J. Yoon, H. Lee and R. Weissleder, *Wiley Interdiscip. Rev.: Nanomed. Nanobiotechnol.*, 2010, **2**(3), 291–304.
2 P. C. Ray, S. A. Sadia Afrin Khan, A. K. Singh, D. Senapati and Z. Fan, *Chem. Soc. Rev.*, 2012, **41**, 3193–3209.
3 J. Kirsch, C. Siltanen, Q. Zhou, A. Revzin and A. Simonian, *Chem. Soc. Rev.*, 2013, **42**, 8733–8768.
4 S. Santra, C. Kaittanis, J. Grimm and J. M. Perez, *Small*, 2009, **5**, 1862–1868.
5 H. Lee, T. J. Yoon and R. Weissleder, *Angew. Chem., Int. Ed. Engl.*, 2009, **48**, 5657–5660.
6 V. Urbanova, M. Magro, A. Gedanken, D. Baratella, F. Vianello and R. Zboril, *Chem. Mater.*, 2014, **26**(23), 6653–6673.
7 H. Lee, E. Sun, D. Ham and R. Weissleder, *Nat. Med.*, 2008, **14**, 869–874.
8 D. Hogemann, V. Ntziachristos, L. Josephson and R. Weissleder, *Bioconjugate Chem.*, 2002, **13**, 116–121.
9 L. R. Skewis, D. Vasiliki and T. J. Lowery, *Encyclopedia of Analytical Chemistry*, 2013.
10 S. Taktak, D. Sosnovik, M. J. Cima, R. Weissleder and L. Josephson, *Anal. Chem.*, 2007, **79**, 8863–8869.

11 Y. Ling, C. C. Vassiliou and M. J. Cima, *Analyst*, 2010, **135**, 2360–2364.
12 J. M. Perez, L. Josephson, T. O'Loughlin, D. Hogemann and R. Weissleder, *Nat. Biotechnol.*, 2002, **20**, 816–820.
13 C. Kaittanis, S. Santra, O. J. Santiesteban, T. J. Henderson and J. M. Perez, *J. Am. Chem. Soc.*, 2011, **133**, 3668–3676.
14 E. J. Werner, A. Datta, C. J. Jocher and K. N. Raymond, *Angew. Chem., Int. Ed.*, 2008, **47**(45), 8568–8580.
15 H. Zhu, J. Fan, B. Wang and X. Peng, *Chem. Soc. Rev.*, 2015, DOI: 10.1039/C4CS00285G.
16 V. C. Pierre, M. J. Allen and P. Caravan, *J. Biol. Inorg. Chem.*, 2014, **19**, 127–131.
17 S. Xue, J. Qiao, F. Pu, M. Cameron and J. J. Yang, *Wiley Interdiscip. Rev.: Nanomed. Nanobiotechnol.*, 2013, 163–179.
18 G. K. Das, Y. Zhang, L. D'Silva, P. Padmanabhan, B. C. Heng, J. S. C. Loo, S. T. Selvan, K. K. Bhakoo and T. T. Y. Tan, *Chem. Mater.*, 2011, **21**, 2439–2446.
19 A. E. Merbach and E. Toth, *The Chemistry of Contrast Agents in Medical Magnetic Resonance Imaging*, John Wiley & Sons, New York, 2001.
20 S. H. Koenig, C. M. Baglin and R. D. Brown 3rd., *Magn. Reson. Med.*, 1985, **2**(3), 283–288.
21 R. A. Moats, S. E. Fraser and T. J. Meade, *Angew. Chem., Int. Ed.*, 1997, **36**, 726–728.
22 V. C. Pierre, M. Melchior, D. M. Doble and K. N. Raymond, *Inorg. Chem.*, 2004, **43**(26), 8520–8525.
23 K. J. Franz and Q. Wang, *Inorg. Chem. Biol.*, 2014, 233–274.
24 C. S. Bonnet and E. Toth, *Chem. Contrast Agents Med. Magn. Reson. Imaging*, 2014, 343–385.
25 A. Datta and K. N. Raymond, *Acc. Chem. Res.*, 2009, **42**(7), 938–947.
26 P. Caravan, *Chem. Soc. Rev.*, 2006, **35**, 512–523.
27 K. Y. Ju, J. W. Lee, G. H. Im, S. Lee, J. Pyo, S. B. Park, J. H. Lee and J. K. Lee, *Biomacromolecules*, 2013, **14**(10), 3491–3497.
28 D. D. Schwert, J. A. Davies and N. Richardson, *Top. Curr. Chem.*, 2002, **221**, 165–199.
29 D. D. Schwert, N. Richardson, G. J. Ji, B. Raduchel, W. Ebert, P. E. Heffner, R. Keck and J. A. Davies, *J. Med. Chem.*, 2005, **48**, 7482–7485.
30 V. Ranc, Z. Markova, M. Hajduch, R. Prucek, L. Kvitek, J. Kaslik, K. Safarova and R. Zboril, *Anal. Chem.*, 2014, **86**(6), 2939–2946.
31 P. Joshi, Y. Zhou, T. Ozkaya Ahmadov and P. Zhang, *J. Mater. Chem. C*, 2014, **2**, 9964–9968.
32 M. Kaya and M. Volkan, *Anal. Chem.*, 2012, **84**(18), 7729–7735.
33 M. Bagherzadeh and M. Heydari, *Analyst*, 2013, **138**, 6044–6051.
34 H. C. Lee, T. H. Chen, W. L. Tseng and C. H. Lin, *Analyst*, 2012, **137**, 5352–5357.
35 C. M. Yu, M. Luo, F. Zeng, F. Y. Zheng and S. Z. Wu, *Chem. Commun.*, 2011, **47**, 9086–9088.
36 Q. Ye, F. Zhou and W. Liu, *Chem. Soc. Rev.*, 2011, **40**, 4244–4258.
37 C. Kaittanis, T. M. Shaffer, A. Ogirala, S. Santra, J. M. Perez, G. Chiosis, Y. Li, L. Josephson and J. Grimm, *Nat. Commun.*, 2014, **5**, 3384.
38 Y. Guo, S. Rogelj and P. Zhang, *Nanotechnology*, 2010, **21**, 065102.
39 R. De Palma, S. Peeters, M. J. Van Bael, H. Van den Rul, K. Bonroy, W. Laureyn, J. Mullens, G. Borghs and G. Maes, *Chem. Mater.*, 2007, **19**, 1821–1831.
40 A. A. Kulkarni, A. A. Weiss and S. S. Iyer, *Anal. Chem.*, 2010, **82**, 7430–7435.
41 S. Bamrungsap, T. Chen, M. I. Shukoor, Z. Chen, K. Sefah, Y. Chen and W. Tan, *ACS Nano*, 2012, **6**, 3974–3981.
42 N. Richardson, J. A. Davies and B. Raduchel, *Polyhedron*, 1999, **18**, 2457–2482.
43 G. T. Hermanson, *Bioconjugate Techniques*, Academic Press, 2nd edn, 2008, p. 1202.
44 D. Dupont, J. Luyten, M. Bloemen, T. Verbiest and K. Koen Binnemans, *Ind. Eng. Chem. Res.*, 2014, **53**(39), 15222–15229.

